Ann Nucl Med (2014) 28:304–313
DOI 10.1007/s12149-014-0813-1

ORIGINAL ARTICLE

^{18}F-FDG PET as a single imaging modality in pediatric neuroblastoma: comparison with abdomen CT and bone scintigraphy

Yun Jung Choi · Hee Sung Hwang · Hyun Jeong Kim · Yong Hyu Jeong · Arthur Cho · Jae Hoon Lee · Mijin Yun · Jong Doo Lee · Won Jun Kang

Received: 7 October 2013 / Accepted: 13 January 2014 / Published online: 31 January 2014
© The Japanese Society of Nuclear Medicine 2014

Abstract
Objective The purpose of this study was to evaluate the diagnostic performance of ^{18}F-fluoro-2-deoxy-D-glucose positron emission tomography (FDG PET) as a single imaging agent in neuroblastoma in comparison with other imaging modalities.
Methods A total of 30 patients with pathologically proven neuroblastoma who underwent FDG PET for staging were enrolled. Diagnostic performance of FDG PET and abdomen CT was compared in detecting soft tissue lesions. FDG PET and bone scintigraphy (BS) were compared in bone metastases. Maximal standardized uptake value (SUVmax) of primary or recurrent lesions was calculated for quantitative analysis.
Results Tumor FDG uptake was detected in 29 of 30 patients with primary neuroblastoma. On initial FDG PET, SUVmax of primary lesions were lower in early stage (I–II) than in late stage (III–IV) (3.03 vs. 5.45, respectively, $p = 0.019$). FDG PET was superior to CT scan in detecting distant lymph nodes (23 vs. 18 from 23 lymph nodes). FDG PET showed higher accuracy to identify bone metastases than BS both on patient-based analyses (100 vs. 94.4 % in sensitivity, 100 vs. 77.8 % in specificity), and on lesion-based analyses (FDG PET: 203 lesions, BS: 86 lesions). Sensitivity and specificity of FDG PET to detect recurrence were 87.5 % and 93.8, respectively.
Conclusion FDG PET was superior to CT in detecting distant LN metastasis and to BS in detecting skeletal metastasis in neuroblastoma. BS might be eliminated in the evaluation of neuroblastoma when FDG PET is performed.

Keywords Neuroblastoma · ^{18}F-fluoro-2-deoxy-D-glucose positron emission tomography (^{18}F-FDG PET) · Bone metastasis · Bone scintigraphy

Introduction

Neuroblastoma is the most common solid extracranial malignancy of childhood [1]. Primary neuroblastoma can arise from the pelvis to the neck [2], but adrenal medulla is the most common primary site for neuroblastoma. In approximately 70 % of patients, metastasis is present at the time of diagnosis and most commonly involves cortical bone and bone marrow (BM). Less frequently, there is involvement of liver, skin, and lung [3, 4]. Accurate staging at the time of diagnosis is the most important factor to determine treatment planning and to predict clinical outcome [5]. Surgical excision is the preferred treatment for localized neuroblastoma. In locally extensive disease, intensive preoperative chemotherapy may be administered. When distant metastases are present, high dose chemotherapy, total body irradiation, and bone marrow reinfusion are beneficial for some children [1, 3].

Because of high incidence of metastasis, diagnostic studies include multiple imaging studies. Ultrasonography (US), chest X-ray, computed tomography (CT), magnetic

Y. J. Choi · H. S. Hwang
Department of Nuclear Medicine, Hallym University Medical Center, Hallym University College of Medicine, Seoul, Korea

H. J. Kim · Y. H. Jeong · A. Cho · J. H. Lee · M. Yun · J. D. Lee · W. J. Kang
Department of Nuclear Medicine, Yonsei University College of Medicine, Seoul, Korea

W. J. Kang (✉)
Division of Nuclear Medicine, Department of Radiology, Yonsei University College of Medicine, Seongsanno 250, Seodaemun-gu, Seoul 120-752, Korea
e-mail: mdkwj@yuhs.ac

resonance imaging (MRI), bone scintigraphy (BS), and metaiodobenzylguanidine (MIBG) scintigraphy are the formally recommended imaging studies [6, 7]. CT has a fundamental role in the evaluation of patient with suspected neuroblastoma. CT is useful for defining the extent of the primary tumor and for evaluating regional or distant lymph node metastases. CT is also important in presurgical assessment of tumor respectability [7–9]. MRI is good for visualization of anatomic details of primary tumor, including relationships with the blood vessels [1, 7–10]. ^{99m}Tc-hydroxymethylene diphosphonate BS is the traditional test to detect bone metastasis. Compared with plain radiographs, BS has superior sensitivity for detecting metastatic sites in bone [11].

MIBG is the guanethidine derivative which is an analog of norepinephrine, and specifically enters neuroendocrine cells. Thus MIBG scintigraphy has played an important role in the assessment of neuroblastoma showing high sensitivity and specificity for identifying bone metastasis and lymph node metastasis. In addition, MIBG scintigraphy allows functional evaluation to differentiate active tumor and post-therapy change. Especially, superior accuracy of MIBG over BS in detecting bone metastasis has been reported [12].

2-[^{18}F] fluoro-2-deoxy-D-glucose positron emission tomography (FDG PET) is a relatively new, useful imaging technique in oncology field [13]. However, it has limited role in pediatric oncology due to problems such as radiation, intravenous access, sedation and bladder catheterization [3, 14, 15]. Despite these problems, FDG PET has many advantages in evaluating both soft tissue and bone metastasis from neuroblastoma. Neuroblastoma and their metastases avidly concentrate FDG before chemotherapy or radiation therapy [16]. Because of higher spatial resolution of the PET scanner and the tomographic nature of PET images, PET was better than BS for detecting small lesions. Therefore, FDG PET can be used to delineate primary tumors, to detect regional and distant metastases and to detect early recurrence. Several studies have compared diagnostic accuracy of FDG PET with MIBG in neuroblastoma. But some studies reported that FDG was better and others reported that MIBG was better [17–19]. FDG PET was found to be most useful in neuroblastoma which fails to accumulate MIBG [16].

FDG PET, MIBG scintigraphy and BS have same advantages in detecting bone metastasis because of whole body assessment. However, it is necessary to omit unnecessary studies to lessen the radiation hazard. There have been some reports that compared FDG PET with MIBG or MIBG with BS, but there are limited studies that compare FDG PET and BS in neuroblastoma. In this study, we attempted to compare the diagnostic accuracy of FDG PET with other imaging modalities in neuroblastoma.

Table 1 Patient characteristics

Patients characteristics	Number
Total	30
Age (years)	
>1.5	13
<1.5	17
Sex	
Male	18
Female	12
Pathology	
Neuroblastoma	28
Ganglioneuroblastoma	2
Treatment	
Surgery and chemotherapy	20
Chemotherapy alone	10
Stage	
I, II	7
III, IV	23

Materials and methods

Patients

This retrospective study was approved by the local institutional review board. Thirty patients (18 males and 12 females; median age 2.7 years) with pathologically proven neuroblastoma were enrolled in a single institute during the period of January 2003–August 2010. All patients underwent pretreatment FDG PET. All patients underwent contrast-enhanced abdomen CT, and 27 patients underwent BS within 14 days of FDG PET. For staging, we used international neuroblastoma staging system (INSS) [20]. Patient characteristics are summarized in Table 1.

Imaging procedure

For FDG PET scan, all patients fasted for at least 4 h and serum glucose levels were less than 140 mg/dl before FDG administration. At 60 min after intravenous injection of FDG, PET scanning was initiated. Images from the neck to the proximal thighs were obtained either on a GE PET scanner with a spatial resolution of 5 mm in the center of the field of view (GE Advance, GE Healthcare) or on a Philips PET system with a spatial resolution of 5.3 mm in the center of the field of view(Allegro, Philips-ADAC Medical Systems). For the GE Advance scanner, approximately 5–10 MBq/kg of FDG was injected IV and PET was performed at 5 min per bed position in a 2D mode. The Allegro scanner acquired data in a 3D mode after the IV administration of 5.18 MBq/kg of FDG. Transmission scans (3 min per bed position) using ^{68}Ge for the GE

Advance scanner or ^{137}Cs for the Allegro scanner were obtained to correct for non-uniform attenuation correction. Transmission scans were interleaved between the multiple emission scans for the Allegro scanner. The obtained images were reconstructed using an iterative reconstruction algorithm, specifically either the ordered-subset expectation maximization (OSEM) for GE Advance or the row-action maximal likelihood algorithm (RAMLA) for Allegro.

The standardized uptake value (SUV) was calculated as follows: SUV = [decay-corrected activity (kBq)/ml of tissue volume]/[injected 18F-FDG activity (kBq)/body mass (g)].The SUV of the lesion was obtained by placing regions of interest (ROI) manually around the lesion and the maximum SUV within an ROI was used to minimize partial volume effects.

BS were performed using a dual-head gamma camera (ADAC Dual Genesys, ADAC Laboratories, Milpitas, CA) equipped with general-purpose collimators. Anterior and posterior whole-body images were acquired approximately 3–4 h after intravenous administration of 9–11 MBq/kg (minimum of 20–40 MBq) of ^{99m}Tc-hydroxymethylene diphosphonate. Additional static planar images were acquired at the discretion of the attending nuclear physician. Single-photon emission computed tomography was not performed routinely.

All patients underwent multi-detector CT scanning (four detector row; Lightspeed Plus, GE Medical Systems, Milwaukee, WI or sixteen-detector row; Sensation 16, Siemens, Erlangen, Germany) according to a following protocol. The parameters were 80 kVp, 155 mA, 5 mm collimation and 10 mm/s table feed. A 60 % iodinated contrast material (Xenetix® 300 injection; Guerbet Asia Pacific) was administered intravenously at a rate of 1–1.5 ml/s using an automatic power injector with a volume of 2 ml/kg, up to a maximum volume of 150 ml. CT scans were obtained 70 s after initiating the contrast material injection, and the abdomen and pelvis, from the level of the hepatic dome to the ischial tuberosities, were scanned with a pitch of 2 and a reconstruction thickness of 2 mm. The transverse images were reconstructed with a soft-tissue algorithm.

Imaging interpretation

Time-matched FDG PET and BS were retrospectively reviewed by two nuclear medicine physicians with 5 and 14 years of experience. The evaluation was conducted visually and without any clinical information. Data regarding anatomic location and type of lesion (soft tissue, LN and bone) were recorded. FDG PET findings were

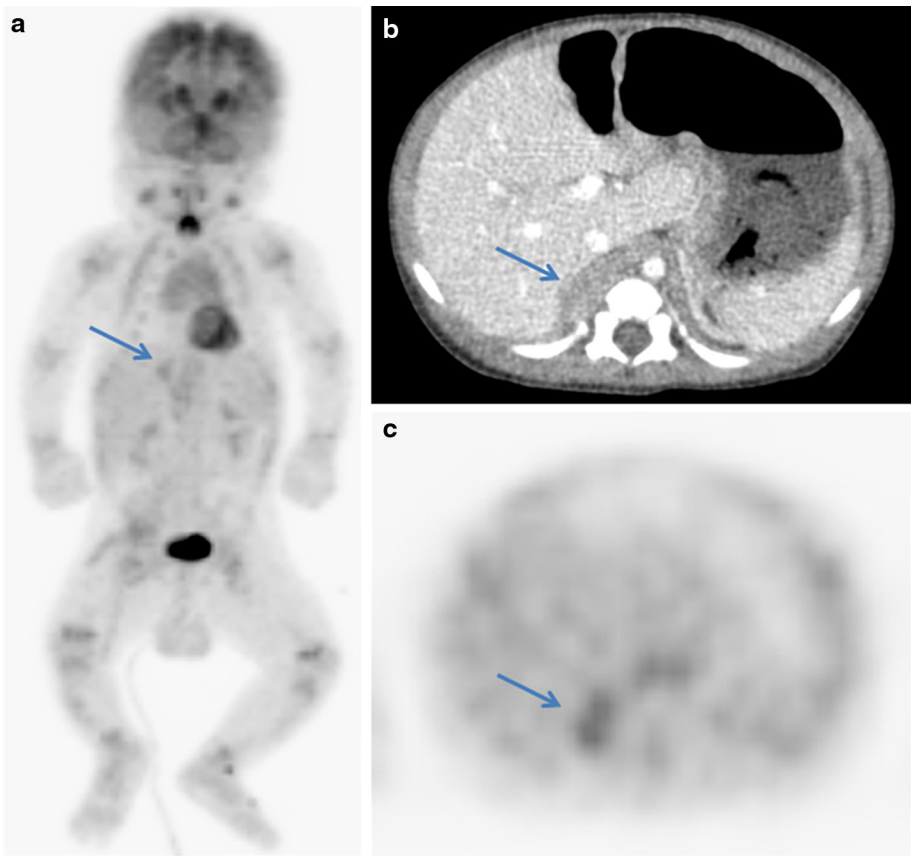

Fig. 1 A 28-day-old boy with stage 1 neuroblastoma. **a** ^{18}F-FDG PET anterior maximum-intensity projection image demonstrates mild uptake at *right upper quadrant* of abdomen. **b** On axial CT image, a mass is seen in *right* paraspinal area. **c** This mass corresponds with hypermetabolic lesion on ^{18}F-FDG PET

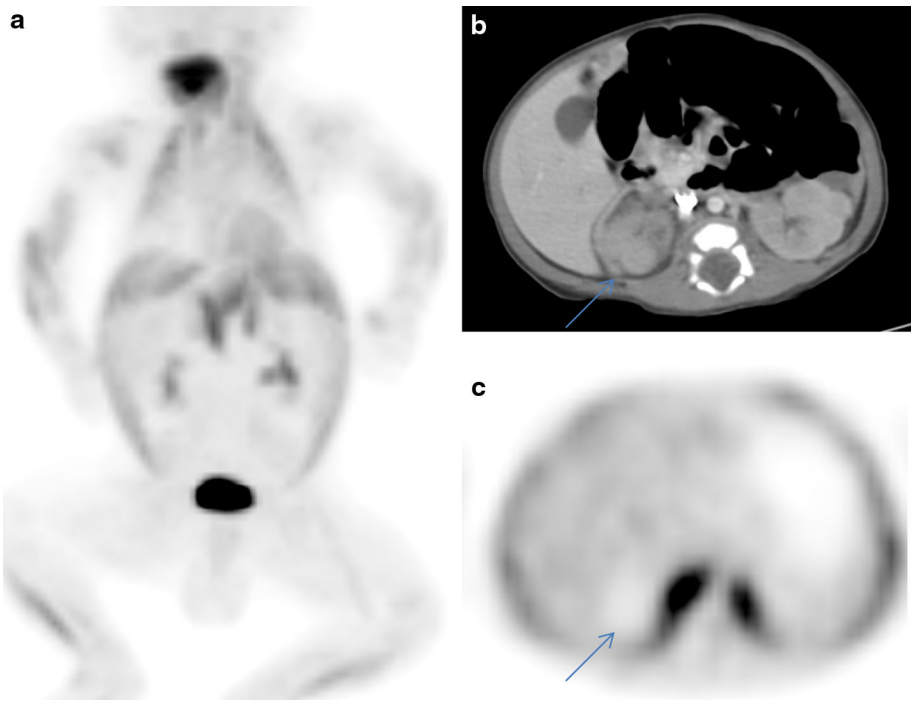

Fig. 2 Images of a 7-day-old boy with stage 1 neuroblastoma. **a** ^{18}F-FDG PET anterior maximum-intensity projection image demonstrates no abnormal focal uptake at abdomen. There are diffuse muscle uptakes, due to crying. **b** About 3-cm-sized mass in the *right* adrenal gland is seen on axial CT image. **c** ^{18}F-FDG PET image shows no definite abnormal hypermetabolism in *right* adrenal gland

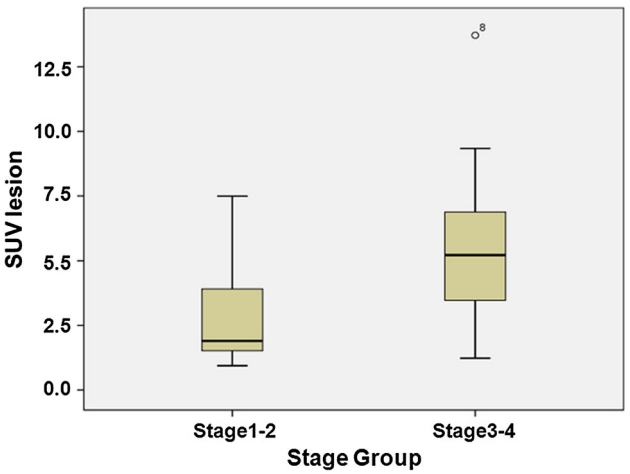

Fig. 3 The distribution of maximum SUV of primary neuroblastoma lesion

considered positive if they demonstrated lesions with increased uptake as compared with background uptake. Positive imaging findings were classified into 4 categories: primary lesion, regional LN, distant LNs, and distant metastasis. All imaging findings were compared with histologic reports and clinical notes. Maximum standard uptake value (SUVmax) was calculated using a manually drawn region of interest (ROI) around the primary lesions.

Skeleton was divided into seventeen categories (C-spine, T-spine, L-spine, sacrum, right pelvic bone, left pelvic bone, right rib cage, left rib cage, sternum, right scapula, left scapula, right humerus, left humerus, right radius/ulna, left radius/ulna, right femur and left femur) and the findings were described according to their location on FDG PET and BS. The definition of abnormal bone uptake was the lesion with higher increased uptake than surrounding bone uptake. To confirm the bone metastases, we analyzed another images such as MRI and evaluated bone marrow biopsy. A lesion was classified 'false-positive' or 'true-negative' if it was not detected on MRI images or got negative result on bone marrow biopsy. A lesion was classified as either 'true-positive' or 'false-negative' if there were matched lesions on MRI images or got negative result on bone marrow biopsy.

We analyzed concordance and discordance of soft-tissue lesions and abnormal LNs on FDG PET and CT. The definition of concordance was a single lesion identified by both modalities (FDG PET and CT) at one time point. And the definition of discordance was identified by one of the two modalities, but not the other at a single time point. To confirm the discordant lesions, we analyzed another images such as MRI, follow-up CT scans or follow-up FDG PET.

Statistical analysis

Independent sample *t* test was used to compare the clinical stage and SUVmax of primary lesions. A p value <0.05 was considered significant. The sensitivity, specificity, positive predictive value (PPV), negative predictive value (NPV) and accuracy of PET/CT were computed for bone metastasis. All analyses were performed using SPSS software (Version 18.0; SPSS Incorporation, Chicago, IL).

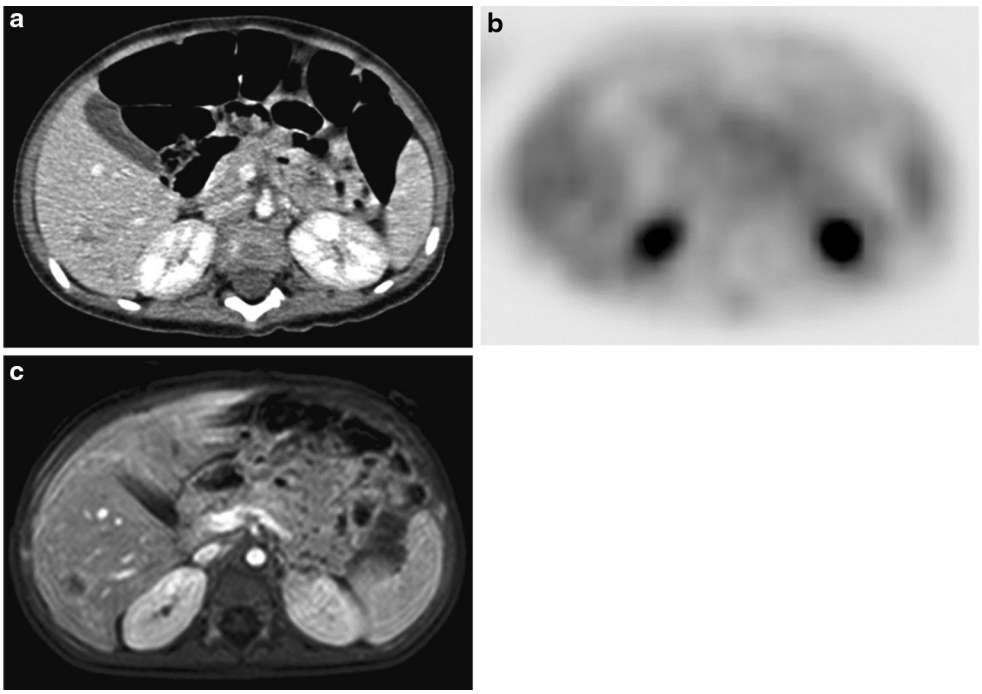

Fig. 4 Image findings of a 14-month-old girl with stage 4 neuroblastoma. **a** ^{18}F-FDG PET anterior maximum-intensity projection image demonstrates intense uptake at *right upper* quadrant of abdomen. **b** Multiple nodules in the *right lower* lung base are seen on axial CT image. **c** ^{18}F-FDG PET image shows no definite abnormal hypermetabolism at lung area. This lesion was confirmed to be lung metastasis from neuroblastoma

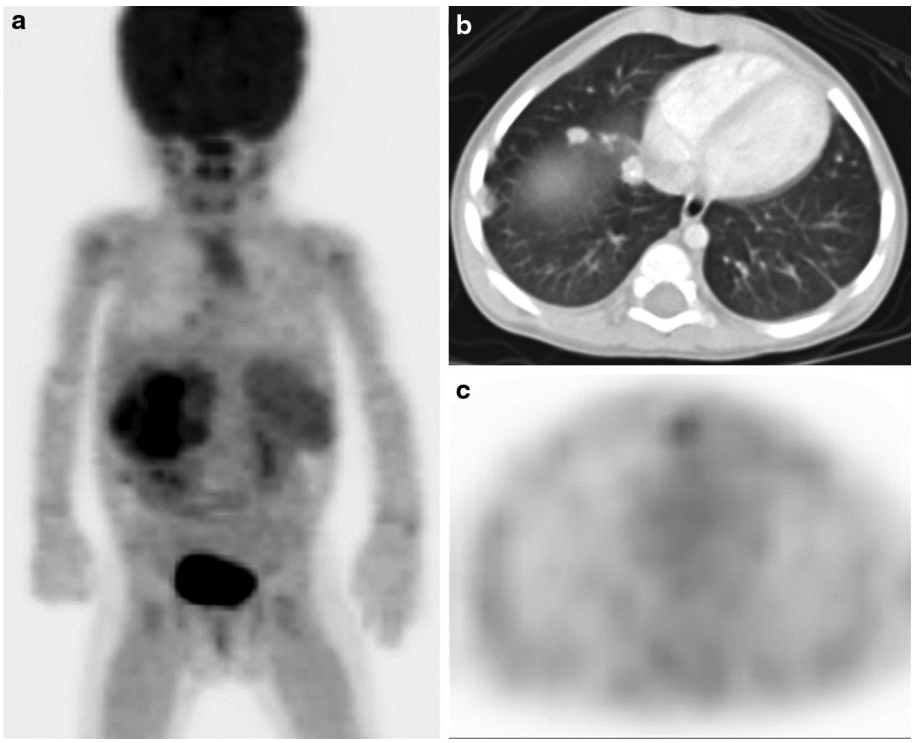

Fig. 5 Image findings of a 13-month-old boy with stage 4 neuroblastoma. **a** On axial CT image, a low attenuation is seen in segment 6 of liver. **b** FDG PET image shows no definite abnormal hypermetabolism at corresponding liver area. **c** On gadolinium-enhanced MRI image, there was a peripheral enhancing nodule in segment 6 of liver. This lesion was confirmed to be metastasis from neuroblastoma

Result

Evaluation of primary sites

FDG PET scans were performed in 30 patients for staging. Twenty-five patients had adrenal mass and 5 patients had retroperitoneal mass. Primary tumor FDG uptake was detected in 29 of 30 primary lesions with sensitivity of 96.7 %. Mean SUVmax of primary sites was 4.89 (range 0.94–13.72) and mean size was 6.25 cm (range 1.7–10.7) (Fig. 1). One false-negative case of FDG PET was 3.1-cm-sized cystic lesion with faint FDG uptake in the right adrenal gland (SUVmax 0.94) (Fig. 2).

Seven of enrolled patients for staging had stage I or II, and 23 patients had stage III or IV. Mean of SUVmax of stage I/II patients was 3.03 (range 0.94–7.49), and that of stage III/IV patients was 5.45 (range 1.23–13.72) (Fig. 3). The SUVmax of stage I/II was significantly lower than that of stage III/IV ($p = 0.019$).

Table 2 ^{18}F-FDG PET and CT in soft-tissue metastasis

	PET positive	PET negative
CT positive	1	2
CT negative	0	27

Evaluation of soft tissue metastasis

There were two cases of confirmed liver metastases and one case of confirmed lung metastasis. In one case, FDG PET revealed multiple hypermetabolic lesions in liver, which were concordant on CT scan (Fig. 4). In other cases, there were discordant lesions with FDG PET negative/CT positive in liver and lung (Fig. 5). A lung metastasis was detected at lung base which imaged on abdomen CT. However, there were no significant abnormal FDG uptakes on PET images. CT tended to be superior to ^{18}F-FDG PET in evaluation of soft tissue metastasis (Table 2).

Evaluation of lymph node metastasis

LN metastases were detected in 24 from 30 patients (80 %). ^{18}F-FDG PET and CT scans showed concordant result to evaluate regional LNs both at ipsilateral and contralateral sites. For the detection of distant LN, CT scan had inferior results to FDG PET. CT scan missed 6 distant LN metastases, which were well detected on FDG PET

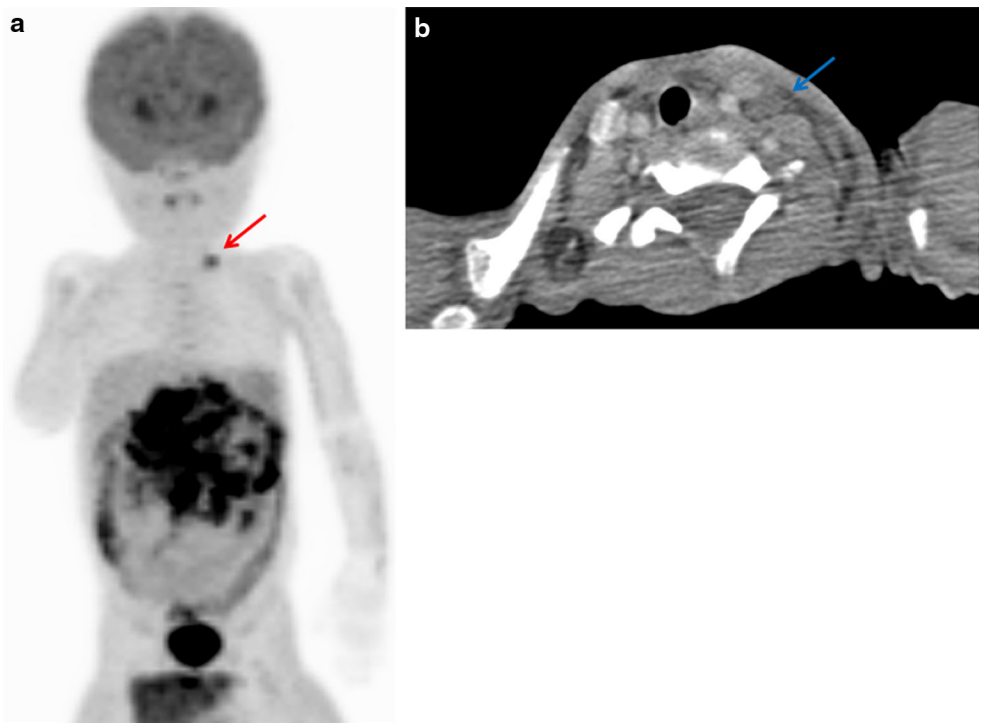

Fig. 6 Images of a 22-month-old boy with stage 3 neuroblastoma. **a** ^{18}F-FDG PET anterior maximum-intensity projection image demonstrates intense uptake at mid abdomen and *left* supraclavicular fossa (*red arrow*). **b** An enhanced chest CT image shows enlarged LN in the *left* supraclavicular fossa (*blue arrow*), which was not imaged at initial abdomen CT. Chest CT was taken after ^{18}F-FDG PET reading. This LN was confirmed to be metastasis (color figure online)

(Fig. 6). When only CT scans were used, 3 of these patients were undervalued in clinical stage (Table 3).

Evaluation of bone metastases

Of 18 patients with confirmed bone metastasis, all patients were identified on FDG PET (Table 4) on patient-based analysis. BS detected 17 patients and missed only one case. Two cases were identified as discordant lesions of BS positive/FDG PET negative. These cases were identified as false positive on additional images such as MRI. On patient base analysis, the sensitivity, specificity, positive predictive value (PPV) and negative predictive value (NPV) of FDG PET were 100, 100, 100 and 100 %, respectively. The sensitivity, specificity, PPV and NPV of BS were 94.4, 77.8, 89.5 and 87.5 %, respectively. Overall accuracy of FDG PET was not significantly higher than of BS ($p = 0.25$).

On lesion base analysis, 203 bone lesions were identified on ^{18}F-FDG PET (Table 5). However, only 86 lesions were detected on ^{99m}Tc-HDP BS. FDG PET detected more metastatic lesions than BS in most cases. Even in concordantly detected cases, most of the lesions were more easily detected and more discernable in FDG PET scans than BS (Fig. 7).

Bone marrow examinations were performed in 29 of the patients. Of these patients, 15 patients were confirmed to have bone metastasis. On FDG PET, there were abnormal spine uptakes in all patients (Table 6), and diffuse uptakes in proximal long bones and pelvic bones were seen in 14 patients. On BS, irregular uptakes of spines were observed in 13 patients and diffuse uptakes in pelvic bones were shown in 12 patients. However, abnormal uptakes in long bones were seen in only 5 patients. The extent of bone marrow involvement was better defined in FDG PET than in BS in all patients.

Table 3 ^{18}F-FDG PET and CT in LN metastases evaluation

	PET positive	PET negative
CT positive	17	1
CT negative	6	6

Table 4 ^{18}F-FDG PET and bone scintigraphy in cortical bone and BM metastases

	TP	TN	FP	FN	Total
FDG PET	18	12	0	0	30
BS	17	7	2	1	27

TP true positive, *TN* true negative, *FP* false positive, *FN* false negative

Table 5 ^{18}F-FDG PET and CT in cortical bone and BM metastases

Patient ID	Numbers of affected skeleton	
	FDG PET	Bone scintigraphy
1	1	1
2	13	2
3	17	14
4	11	5
6	0	1 (FP)
8	2	0
9	1	1
13	0	1 (FP)
14	11	1
15	14	3
17	9	4
18	17	14
19	11	7
20	9	5
21	2	1
24	17	6
26	17	5
27	17	7
28	17	4
29	17	4
Total	203	86

FP false positive

Discussion

This study demonstrates that FDG PET is superior to CT in detecting distant lymph nodes and to BS in detecting bone metastasis in pediatric neuroblastoma.

In our 30 patients for staging work-up, most primary lesion and metastatic LNs were FDG avid. CT and FDG PET had similar results to evaluate primary lesions and regional LN metastases. However, FDG PET had better result than CT to evaluate distant LN metastases, which was due to the result of whole body screening. CT often missed the distant LNs such as supraclavicular LNs. However, in patients with hepatic or pulmonary metastasis, CT had superior result to FDG PET. FDG PET missed 1 liver metastasis and 1 lung metastasis. These false negatives can undervalue clinical stage of disease and might influence treatment plans. In our study, most of the patients did not undergo FDG PET/CT but underwent FDG PET. PET/CT had been shown to be superior to PET alone due to anatomic information of CT scan [21]. Therefore, using the PET/CT, the sensitivity and specificity of distant metastasis will be improved.

Our results showed that primary neuroblastoma with low stages had lower SUVmax than that with higher stages.

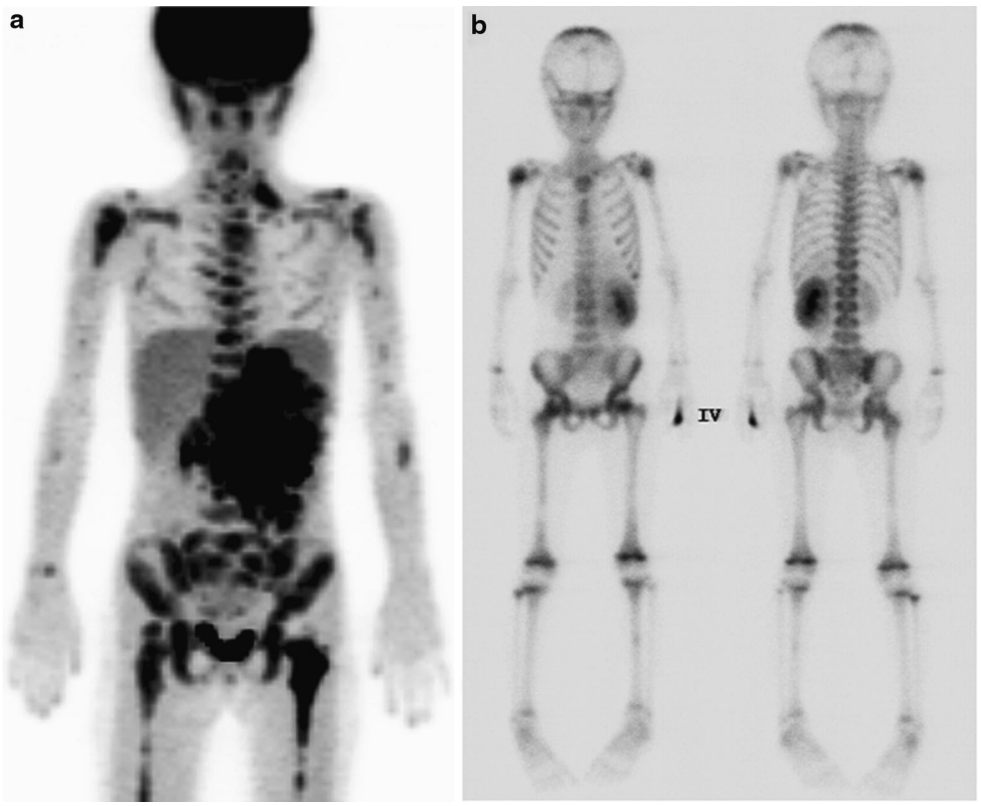

Fig. 7 Images of a 5-year-old girl with stage 4 neuroblastoma. This patient was confirmed bone metastases by bone marrow biopsy at bilateral iliac crests. **a** ^{18}F-FDG PET anterior maximum-intensity projection image demonstrates diffuse intense uptake in axial and proximal appendicular skeleton. **b** Anterior and posterior bone scintigraphy demonstrates focally increased uptake in the skull, *right* proximal humerus, *left* distal femur and *left* tibia. Skull and tibia were not imaged on PET scan, but other lesions were more easily detected in FDG PET images

Table 6 Abnormal uptake in patient with bone metastasis

	Bone scintigraphy	FDG PET
Spine	13	15
Long bone	5	14
Pelvis	12	14

There was a study about correlation of FDG PET findings and disease status of neuroblastoma [17]. FDG PET findings correlated well with disease status as determined by standard imaging modalities, BM biopsy, urine vanillylmandelic acid (VMA) and homovanillic acid (HVA) levels and clinical history. FDG uptake is directly proportional to tumor burden and to tumor cell proliferation. Thus, maximal SUV of primary lesion can reflect the aggressiveness of tumor and have some relationship with prognosis.

Recently, the role of BS in neuroblastoma had reduced because of superior sensitivity of MRI and FDG PET in evaluating bone metastasis from neuroblastoma. Several studies had shown that BS was less sensitive to detect bone metastases than MRI in pediatric malignancy [22, 23]. In other studies, FDG PET was superior to BS in the detection of osteolytic bone lesions in breast cancer and BM metastases in melanoma [24, 25]. However, there were limited clinical researches to compare FDG PET and BS for detecting bone metastases in patients with neuroblastoma. Kushner et al. [17] showed that FDG PET identified more osteomedullary abnormalities than BS. In our study, FDG PET was superior to BS for detecting bone metastases. Physiologic uptake of FDG in the BM may give false-positive result in staging of neuroblastoma [4]. However, clinical history and physical examination can help prevent misinterpretation of FDG PET finding. BS has been thought to be sensitive to detect cortical bone metastasis from neuroblastoma. However, on both patient-based analyses and lesion-based analysis, there was no case where BS identified more lesions than FDG PET in the present study. Therefore, FDG PET might replace BS to identify cortical bone and BM metastases in neuroblastoma.

We compared FDG PET and BS by means of 17 regional categories, which did not contain skull and tibia.

Figure 7 showed the case of diffuse bone metastases involving skull and left tibia, which were not covered in FDG PET image. Routine FDG PET protocol recommends the image acquisition from skull base to thigh. To overcome this pitfall, image acquisition from head to feet should be considered.

In this study, FDG PET revealed more distant lymph nodes than abdomen CT. Due to the advantage of whole body screening, nuclear imaging studies including FDG PET show high detection rate in distant lymph node metastasis in many tumors [26–28]. One example is supraclavicular lymph node. Detection rate of CT in supraclavicular lymph node is relatively low, and its limited value has been reported in many malignancies [29]. However, FDG PET showed high detection rate in supraclavicular lymph node in the present study. FDG PET is expected to be useful in detecting distant lymph node metastasis in neuroblastoma.

In pediatric oncologic fields, imaging evaluation is performed repetitively with a relatively short time interval. There are several problems from repetitive imaging studies. First, children are more radiosensitive than adults [3]. Therefore, reducing radiation dose is important in pediatric oncology. Radiation exposure from FDG PET may be diminished by frequent voiding [15], but more fundamental method to reduce radiation exposure will be necessary. Second, children may need sedation/anesthesia for FDG PET just as other procedure in pediatric radiology. Young children, typically under 4–6 years of age, may require conscious sedation or even general anesthesia to insure they remain stationary during the entire imaging acquisition [30]. For those reasons, studies to assess feasibility to reduce the number of the studies, without compromising patient care, are crucial. In the present study, we suggest that BS might be eliminated from the routine protocol in case FDG PET is performed. Contrary to our initial assumption that BS has clinical role in bone cortex metastasis, there was little cases where BS is superior to FDG PET. Although more large-scale studies with prospective design will be needed before excluding BS among initial tests of neuroblastoma, our result is consistent with previous studies that compared BS with MIBG or FDG PET [17].

There were several limitations in the present study. First of all, this study had relatively small sample size. Neuroblastoma accounts for 7.6 % of all childhood cancer and the prevalence is approximately one in 10,000 live births which would generate about 525 newly diagnosed cases annually [1, 31]. However, the absolute number of neuroblastoma patient is small in general population. Second, there was no comparison to MIBG scintigraphy. MIBG is the nuclear imaging method of choice for neuroblastoma, which has shown high diagnostic accuracy to evaluate initial staging and to identify residual and recurrent lesions. Several studies compared FDG PET with MIBG scintigraphy. These studies had shown that FDG PET had superior results to MIBG scintigraphy in patients with lower stage neuroblastoma but cannot replace MIBG scintigraphy in high-risk neuroblastoma [2, 18, 32, 33]. However, the supply of ^{123}I-MIBG was not available until recent years in our hospital. Therefore, most patients could not undergo MIBG scintigraphy.

Conclusion

The present study demonstrated that FDG PET was helpful in evaluating initial tumor stage in patients with neuroblastoma. FDG PET was superior to BS in detecting bone metastases, and to CT in detecting distant LN metastasis. FDG PET might substitute for BS to evaluate bone metastases to reduce the radiation exposure in pediatric neuroblastoma patients.

Acknowledgments This study was supported by the National Research Foundation of Korea Grant funded by the Korean Government (National Research Foundation of Korea, NRF-2011-013-E00038, NRF-2012R1A1A2041563 and No. 2012027276).

References

1. Haase GM, Perez C, Atkinson JB. Current aspects of biology, risk assessment, and treatment of neuroblastoma. Semin Surg Oncol. 1999;16:91–104.
2. Taggart DR, Han MM, Quach A, Groshen S, Ye W, Villablanca JG, et al. Comparison of iodine-123 metaiodobenzylguanidine (MIBG) scan and [18F]fluorodeoxyglucose positron emission tomography to evaluate response after iodine-131 MIBG therapy for relapsed neuroblastoma. J Clin Oncol. 2009;27:5343–9.
3. Jadvar H, Connolly LP, Fahey FH, Shulkin BL. PET and PET/CT in pediatric oncology. Semin Nucl Med. 2007;37:316–31.
4. Kumar R, Shandal V, Shamim SA, Halanaik D, Malhotra A. Clinical applications of PET and PET/CT in pediatric malignancies. Expert Rev Anticancer Ther. 2010;10:755–68.
5. Hormann M. Neuroblastoma in children. Radiologe. 2008;48:940–5.
6. Ley S, Ley-Zaporozhan J, Gunther P, Deubzer HE, Witt O, Schenk JP. Neuroblastoma imaging. Rofo. 2011;183:217–25.
7. Kushner BH. Neuroblastoma: a disease requiring a multitude of imaging studies. J Nucl Med. 2004;45:1172–88.
8. Stark DD, Moss AA, Brasch RC, de Lorimier AA, Albin AR, London DA, et al. Neuroblastoma: diagnostic imaging and staging. Radiology. 1983;148:101–5.
9. Mullassery D, Dominici C, Jesudason EC, McDowell HP, Losty PD. Neuroblastoma: contemporary management. Arch Dis Child Educ Pract Ed. 2009;94:177–85.
10. Siegel MJ, Ishwaran H, Fletcher BD, Meyer JS, Hoffer FA, Jaramillo D, et al. Staging of neuroblastoma at imaging: report of the radiology diagnostic oncology group. Radiology. 2002;223:168–75.
11. Heisel MA, Miller JH, Reid BS, Siegel SE. Radionuclide bone scan in neuroblastoma. Pediatrics. 1983;71:206–9.

12. Sharp SE, Gelfand MJ, Shulkin BL. Pediatrics: diagnosis of neuroblastoma. Semin Nucl Med. 2011;41:345–53.
13. Kleis M, Daldrup-Link H, Matthay K, Goldsby R, Lu Y, Schuster T, et al. Diagnostic value of PET/CT for the staging and restaging of pediatric tumors. Eur J Nucl Med Mol Imaging. 2009;36:23–36.
14. Shulkin BL. PET imaging in pediatric oncology. Pediatr Radiol. 2004;34:199–204.
15. Shore RM. Positron emission tomography/computed tomography (PET/CT) in children. Pediatr Ann. 2008;37:404–12.
16. Shulkin BL, Hutchinson RJ, Castle VP, Yanik GA, Shapiro B, Sisson JC. Neuroblastoma: positron emission tomography with 2-[fluorine-18]-fluoro-2-deoxy-D-glucose compared with metaiodobenzylguanidine scintigraphy. Radiology. 1996;199:743–50.
17. Kushner BH, Yeung HW, Larson SM, Kramer K, Cheung NK. Extending positron emission tomography scan utility to high-risk neuroblastoma: fluorine-18 fluorodeoxyglucose positron emission tomography as sole imaging modality in follow-up of patients. J Clin Oncol. 2001;19:3397–405.
18. Sharp SE, Shulkin BL, Gelfand MJ, Salisbury S, Furman WL. 123I-MIBG scintigraphy and 18F-FDG PET in neuroblastoma. J Nucl Med. 2009;50:1237–43.
19. Melzer HI, Coppenrath E, Schmid I, Albert MH, von Schweinitz D, Tudball C, et al. (1)(2)(3)I-MIBG scintigraphy/SPECT versus (1)(8)F-FDG PET in paediatric neuroblastoma. Eur J Nucl Med Mol Imaging. 2011;38:1648–58.
20. Brodeur GM, Pritchard J, Berthold F, Carlsen NL, Castel V, Castelberry RP, et al. Revisions of the international criteria for neuroblastoma diagnosis, staging, and response to treatment. J Clin Oncol. 1993;11:1466–77.
21. Nanni C, Rubello D, Castellucci P, Farsad M, Franchi R, Rampin L, et al. 18F-FDG PET/CT fusion imaging in paediatric solid extracranial tumours. Biomed Pharmacother. 2006;60:593–606.
22. Goo HW, Choi SH, Ghim T, Moon HN, Seo JJ. Whole-body MRI of paediatric malignant tumours: comparison with conventional oncological imaging methods. Pediatr Radiol. 2005;35:766–73.
23. Mentzel HJ, Kentouche K, Sauner D, Fleischmann C, Vogt S, Gottschild D, et al. Comparison of whole-body STIR-MRI and 99mTc-methylene-diphosphonate scintigraphy in children with suspected multifocal bone lesions. Eur Radiol. 2004;14:2297–302.
24. Abe K, Sasaki M, Kuwabara Y, Koga H, Baba S, Hayashi K, et al. Comparison of 18FDG-PET with 99mTc-HMDP scintigraphy for the detection of bone metastases in patients with breast cancer. Ann Nucl Med. 2005;19:573–9.
25. Aydin A, Yu JQ, Zhuang H, Alavi A. Detection of bone marrow metastases by FDG-PET and missed by bone scintigraphy in widespread melanoma. Clin Nucl Med. 2005;30:606–7.
26. Aukema TS, Straver ME, Peeters MJ, Russell NS, Gilhuijs KG, Vogel WV, et al. Detection of extra-axillary lymph node involvement with FDG PET/CT in patients with stage II-III breast cancer. Eur J Cancer. 2010;46:3205–10.
27. Graafland NM, Leijte JA, Valdes Olmos RA, Hoefnagel CA, Teertstra HJ, Horenblas S. Scanning with 18F-FDG-PET/CT for detection of pelvic nodal involvement in inguinal node-positive penile carcinoma. Eur Urol. 2009;56:339–45.
28. Yun M, Lim JS, Noh SH, Hyung WJ, Cheong JH, Bong JK, et al. Lymph node staging of gastric cancer using (18)F-FDG PET: a comparison study with CT. J Nucl Med. 2005;46:1582–8.
29. Lee JH, Kim J, Moon HJ, Cho A, Yun M, Lee JD, et al. Supraclavicular lymph nodes detected by 18F-FDG PET/CT in cancer patients: assessment with 18F-FDG PET/CT and sonography. AJR Am J Roentgenol. 2012;198:187–93.
30. Nadel HR, Shulkin B. Pediatric positron emission tomography-computed tomography protocol considerations. Semin Ultrasound CT MR. 2008;29:271–6.
31. Kaatsch P. Epidemiology of childhood cancer. Cancer Treat Rev. 2010;36:277–85.
32. Nguyen NC, Bhatla D, Osman MM. 123I-MIBG scintigraphy and 18F-FDG PET in neuroblastoma. J Nucl Med. 2010;51:330–1 (author reply 1).
33. Papathanasiou ND, Gaze MN, Sullivan K, Aldridge M, Waddington W, Almuhaideb A, et al. 18F-FDG PET/CT and 123I-metaiodobenzylguanidine imaging in high-risk neuroblastoma: diagnostic comparison and survival analysis. J Nucl Med. 2011;52:519–25.